This is not a peer-reviewed article.
Food Processing Automation Conference CD-Rom. Proceedings of the 28-29 June 2008 Conference (Providence, Rhode Island)
Publication date 28 June 2008
ASABE Publication Number 701P0508cd

Detection of bacterial biofilm on stainless steel by hyperspectral fluorescence imaging

Won Jun, Ph.D.

Food Safety Laboratory, U.S. Department of Agriculture, Agricultural Research Service, Bldg. 303, BARC-East, 10300 Baltimore Avenue, Beltsville, MD 20705, USA

Kangjin Lee, Ph.D.

Nondestructive Quality Evaluation Laboratory, Rural Development Administration, 249 Seodundong, Kwonseongu, Suwon, 441-100, Republic of Korea

Patricia Millner, Ph.D.

Food Safety Laboratory, U.S. Department of Agriculture, Agricultural Research Service, Bldg. 303, BARC-East, 10300 Baltimore Avenue, Beltsville, MD 20705, USA

Manan Sharma, Ph.D.

Food Safety Laboratory, U.S. Department of Agriculture, Agricultural Research Service, Bldg. 303, BARC-East, 10300 Baltimore Avenue, Beltsville, MD 20705, USA

Kuanglin Chao, Ph.D.

Food Safety Laboratory, U.S. Department of Agriculture, Agricultural Research Service, Bldg. 303, BARC-East, 10300 Baltimore Avenue, Beltsville, MD 20705, USA

Moon S. Kim, Ph.D.

Food Safety Laboratory, U.S. Department of Agriculture, Agricultural Research Service, Bldg. 303, BARC-East, 10300 Baltimore Avenue, Beltsville, MD 20705, USA

Abstract. In this study, hyperspectral fluorescence imaging techniques were investigated for detection of microbial biofilm on stainless steel plates typically used to manufacture food processing equipment. Stainless steel coupons were immersed in bacterium cultures of nonpathogenic E. coli, Pseudomonas pertucinogena, Erwinia chrysanthemi, and Listeria innocua. Following a 1-week growth in rich medium tryptic soy broth (TSB) and M9 minimal medium with casamino acids (M9C), biofilm formations were evaluated using a recently developed portable hyperspectral fluorescence imaging system. Hyperspectral fluorescence images of the biofilm samples, in response to ultraviolet-A (320 to 400 nm) excitation, were acquired from 416 to 700 nm. Fluorescence images in the blue emission peak region exhibited the most contrast between biofilms and stainless steel coupons. On the basis of correlation analyses, two-band ratios compared with the single-band images enhanced the contrast between the biofilm forming area and untreated coupon surfaces. A two-band fluorescence ratio image, 444/588 nm, resulted in the greatest contrast between the biofilm formations and stainless steel coupon for the biofilms grown in M9C medium. TSB medium showed relatively high auto-fluorescence, and thus further investigation is needed to mitigate the contribution of strong TSB auto-fluorescence in detection of biofilms.

Keywords. Hyperspectral imaging, Fluorescence, Bacterial contamination, Biofilm, Detection

1. Introduction

Biofilms, the slime substances that form on the surface of food processing equipment, are harbor sites for micro-organisms. The fact that pathogens can form biofilms makes them a real concern for the food processing industry (Kumar et al., 1998). Bacteria can attach to a surface such as the stainless steel typically used in the manufacture of food processing equipment, and secrete polysaccharide-like substance that adheres the cells to the surface and to one another. Within 24 hours, the organisms can establish a community of biofilms. This can potentially lead to cross-contamination of food product through cell

sloughing (Chmielewski et al., 2003). The establishment of the biofilms enhances microorganism activity and forms a protective shield allowing the organisms to be less susceptible to environmental stress such as starvation or heavy metals. It has also been shown that bacteria attached to surfaces show greater resistance to disinfection (Keevil, 2002). The occurrence of biofilm contamination on food processing equipment suggests that sanitation procedures during food processing operations may be inadequate. Hence, there is a need to develop rapid detection methods for biofilm formation for effective sanitation and to prevent potential cross-contamination problems in food processing environments.

Researchers at the Food Safety Laboratory, Agricultural Research Service (ARS), USDA have developed imaging techniques as potential tools for quality and safety inspection of a variety of agricultural food products (Kim et al., 2001; Kim et al., 2002; Kim et al., 2003; Kim et al, 2005; Vargas et al., 2005). We recently developed a line-scan (push-broom) based, portable hyperspectral imaging system capable of reflectance and fluorescence measurements. In this study, we demonstrated the potential of fluorescence imaging technique for detection of microbial biofilms on stainless steel coupons.

2. Materials and methods

2.1 Samples

E. coli O157:H7 strains 3704 and CDC B6-914, *E. coli* strains MW423, MW416, MW425, and ECRC 99.1232, *Pseudomonas pertucinogena*, *Erwinia chrysanthemi*, and *Listeria innocua* were grown in 15 ml of both M9 medium with casamino acids (Difco Laboratories, Detroit, MI) and TSB (Difco) media respectively in 50-ml falcon conical tubes at 37°C for 1 day, then a sterile coupon (2 by 5 cm) was deposited in this culture, and were incubated at 37°C in static condition for 6 days for biofilm formation. M9 medium with casamino acids (M9C) was prepared as described by ATCC medium 1281 (www.atcc.org) and included per liter: 200 ml of M9 minimal salts, 5x; Casamino acids 5 g; Na_2HPO_4 6g; KH_2PO_4 3 g; NaCl 0.5g; NH_4Cl 1g; 1 ml of 1M $MgSO_4$; 10 ml 1 mg/ml thiamine; 1 ml $CaCl_2$ (0.1 M). All experiments were replicated four times.

2.1 Portable Hyperspectral Fluorescence Imaging System

The portable hyperspectral imaging system (Fig 1.) utilizes an electron-multiplying charge-coupled-device (EMCCD: Luca R, ANDOR Technology, South Windsor, CT, USA). The EMCCD consists of a 1002 X 1004 array of pixels (each 8 X 8 μm) and is thermoelectrically cooled to -20°C. It operates at a maximum of 12.5 MHz pixel-readout rate and image data is digitized in 14-bit. An imaging spectrograph (VNIR Concentric Imaging Spectrograph, Headwall photonics, Fitchburg, Massachusetts) and a C-mount lens (Rainbow CCTV S6X11, International Space Optics, S.A., Irvine, CA, USA) are attached to the EMCCD. The Instantaneous Field Of View (IFOV) is limited to a thin line by the spectrograph aperture slit (25 μm). Through the slit, light from the scanned line is dispersed by a concentric grating and projected onto the EMCCD. Therefore, for each line-scan, a two-dimensional (spatial and spectral) image is created with spatial along the horizontal axis and spectral along the vertical axis of the EMCCD. For fluorescence imaging, the sample illumination is provided by a pair of UV-A lamps (365 nm, EN-280 L/12, Spectronics Corp., Westbury, NY, USA).

For this investigation using the fluorescence imaging technique, the vertical pixels (spectral) were binned by 6, resulting in a total of 60 channels spanning from 416 nm to 700 nm with a spectral increment of approximately 4.79 nm per channel. Thus, fluorescence spectra obtained by the imaging system are presented from 416 to 700 nm.

With the use of SDK (Software Development Kit) provided by the EMCCD manufacturer, interface software for imaging system control and data acquisition was developed on a MS Windows Visual Basic (Version 6.0) platform. We also developed image processing and analysis software using a MS Windows Visual Basic platform.

3. Results

Figure 2 shows the fluorescence spectra from 416 to 700 nm extracted from the hyperspectral images of bacterial biofilms on stainless steel coupons. Each spectrum represents an average of 20 individual spectra, each obtained from a single pixel location (5 per stainless coupon) from the hyperspectral image data. Microbial biofilms grown in M9C minimal medium showed considerably high fluorescence emission

intensities in the blue regions (~ 480 nm) compared to control M9C medium on stainless steel coupon, with the UV-A excitation (Figure 2a). The emission spectra from biofilms grown in TSB medium exhibited relatively higher fluorescence at also around 480 nm than those grown in M9C (Figure 2b). Furthermore, control TSB medium on stainless steel background exhibited fluorescence emission intensities nearly identical to those of the biofilms. These observations indicated that further investigation is needed to mitigate (and differentiate) the contribution of strong TSB auto-fluorescence in detection of biofilms.

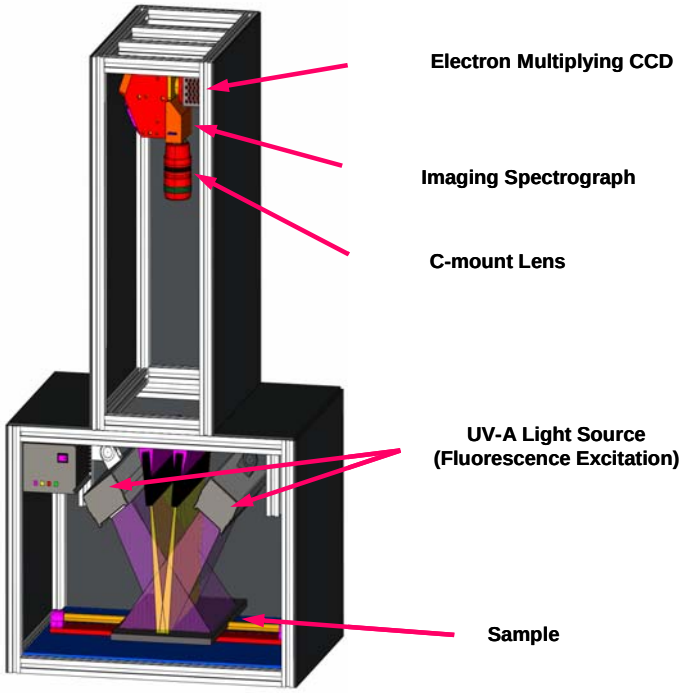

Figure 1. Portable hyperspectral fluorescence imaging system.

Figure 3 is a contour plot of the correlation coefficients for the two-wavelength ratios. The correlation analyses were conducted using a total of 120 individual spectra where 60 spectra were randomly extracted from the biofilm regions and anoother 60 from the medium-only regions. The highest correlation coefficient (r) of 0.85 occurred at 444 nm and 588 nm for the M9C-based biofilms on stainless steel coupons (Figure 3a) whereas the highest correlation coefficient was observed at 473 nm and 645 nm with r = -0.54 for biofilm formations in TSB medium. The low value of correlation coefficient for TSB grown biofilms is indicated that there is no relation between biofilm formation and TSB medium. As discussed earlier, because of the strong TSB auto-fluorescence, the two-wavelength fluorescence ratio method may not allow differentiation of biofilms and TSB medium (Figure 3b).

Results from fluorescence ratio image (444/588 nm) of the M9C minimal medium grown biofilm samples are shown in Figure 4a. We observed that biofilms were developed above medium-air interface, indicating that cells crawled over medium fill line on stainless steel surfaces and produced biofilm. Control M9C medium showed minimal fluorescence on stainless steel coupons. Fluorescence ratio (and individual wavelengths) responses for biofilms were much higher when biofilms were formed in TSB medium (Figure 4b). Based on the image of biofilm formation areas, it appeared that different types of growth medium might have an effect on biofilm formation and accumulation. Thus, biofilm formation might be dependent

on growth medium type. Consistent with this observation, Reisner et al. (2006) noted that growth medium composition had a significant impact on biofilm-forming capability. The complex nutrient-rich medium

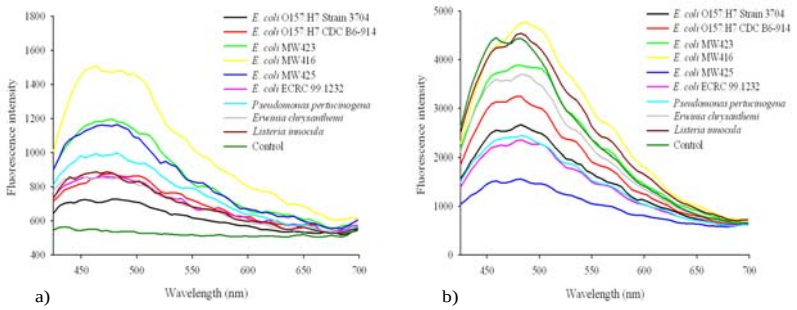

Figure 2. Fluorescence spectra of biofilms extracted from the hyperspectral image data where each spectrum represents a mean of 20 spectra (5 pixels/coupon X 4 coupons). Fluorescence spectra of biofilms formed in M9C medium (a) and TSB medium (b). Control indicates medium only on stainless steel coupons.

(TSB) showed aggregated biofilm formations on coupons compared to sporadic biofilm formations in M9C medium. The control coupons with TSB medium exhibited relatively strong auto-fluorescence and thus, it was difficult to differentiate the TSB medium and bacterial biofilms in the ratio images (figure 4b).

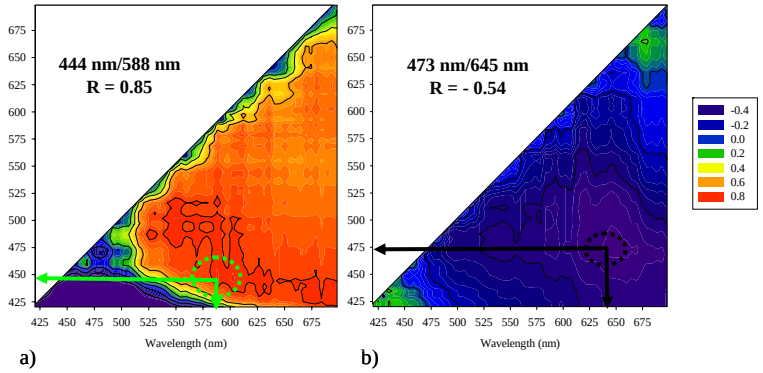

Figure 3. Contour plots of the correlation coefficients for the two-wavelength ratios. Biofilm formation on stainless steel coupon in M9C (a) and TSB (b) media.

4. Conclusion

In this paper, we presented preliminary results using the recently developed portable hyperspectral imaging system for detection of microbial biofilms on stainless steel coupons, mainly based on a fluorescence imaging method. A two-band fluorescence ratio using emission bands at 444 nm and 588 nm (444/588 nm) enhanced biofilm features on stainless steel coupons. However, we could not separate biofilm formations from medium when the biofilms were formed in TSB medium. This was due to the strong auto-fluorescence emanating from the TSB medium. However, detecting the presence of medium-like substances as a potential harbor site for microbial growth may also be useful as an indirect means to reduce potential food safety risks. Our results suggested that two-band fluorescence ratios can be used to develop a portable food safety inspection system for sanitation monitoring of food processing equipment surfaces.

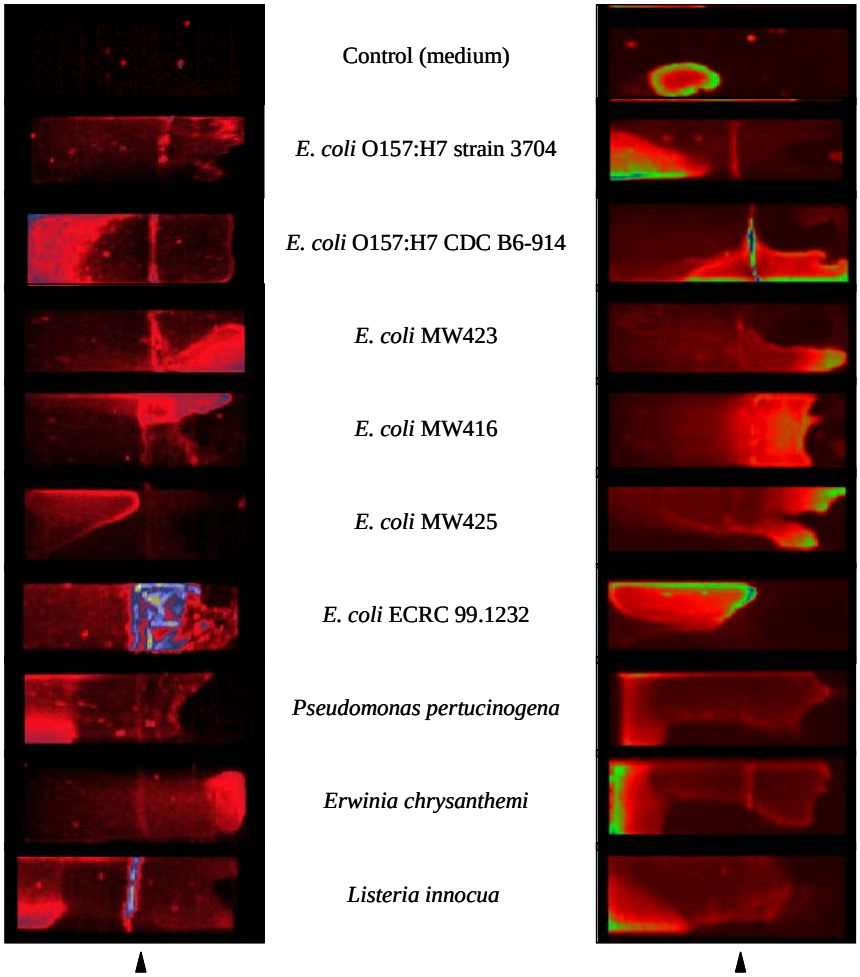

Figure 4. Fluorescence ratio images (a: 444/588 nm, b: 473/645 nm) of biofilm formations on stainless steel coupons in M9C (a) and TSB (b) media acquired with the portable hyperspectral imaging system. Coupons were submerged in 50-ml tubes containing 15 ml of medium for a 1-week at 37ºC. The arrowheads indicate the medium fill lines.

5. References

Chmielewski, R.A.N. and J.F. Frank. Biofilm Formation and Control in Food Processing Facilities, Comp. Rev. Food Sci. Food Safety. Vol (2):22-32 (2003).

Keevil, C.W. Pathogens in environmental biofilms, p. 2339-2356. *In* G. Bitton (ed.), Encyclopedia of environmental microbiology. Wiley, New York, NY (2002).

Kumar, C.G. and S.K. Anand. Significance of microbial biofilms in food industry: a review, Int. J. Food Microbiol. Vol (42):9-27 (1998).

Kim, M.S., A.M. Lefcourt, and Y.R., Chen. Optical fluorescence excitation and emission bands for detection of fecal contamination. J. Food Protect. 66(7):1198-1207 (2003).

Kim, M.S., Y.R. Chen, and P.M. Mehl. Hyperspectral reflectance and fluorescence imaging system for food quality and safety. Trans. of ASAE 44, 721-729 (2001).
Kim, M.S., A.M. Lefcourt, Y.R. Chen, I. Kim, K. Chao, and D. Chan. Multispectral detection of fecal contamination on apples based on hyperspectral imagery-part II: Application of fluorescence imaging. Trans. ASAE. 45(6):2039-2047 (2002).
Kim, M.S., A.M. Lefcourt, Y.R. Chen, and T. Yang. Automated detection of fecal contamination of apples based on multispectral fluorescence image fusion. J. Food Engineering. 71(1):85-91 (2005).
Reisner, A., K.A. Krofgelt, B.M. Klein, E.L. Zechner, and S. Molin. In vitro biofilm formation of commensal and pathogenic Escherichia coli strains. J. Bacteriol. Vol 188(10): 3572-3581 (2006).
Vargas, A.M., M.S. Kim, Y. Tao, A.M. Lefcourt, Y.R. Chen, Y. Luo, Y. Song, and R. Buchanan. Detection of fecal contamination on cantaloupes using hyperspectral fluorescence imagery. J. Food Science. 70(8):E471-E476 (2005).
www.atcc.org/mediapdfs/1281.pdf